Article:

Dobakhshari, AS, Abdolmaleki, M, Terzija, V et al. (1 more author) (2020) Online Non-iterative Estimation of Transmission Line and Transformer Parameters by SCADA Data. IEEE Transactions on Power Systems. ISSN 0885-8950

https://doi.org/10.1109/TPWRS.2020.3037997

Online Non-iterative Estimation of Transmission Line and Transformer Parameters by SCADA Data

A. S. Dobakhshari, *Member, IEEE,* V. Terzija, *Fellow, IEEE,* and S. Azizi, *Senior Member, IEEE*

***Abstract*—Utilization of abundant measurements provided by supervisory control and data acquisition (SCADA) system has attracted increasing attention. Real-time estimation of transmission line parameters, utilizing voltage and power flow measurements provided by remote terminal units (RTUs) located at two substations across the line, has been investigated, recently. This paper improves this approach by introducing a novel exact linear reformulation of the problem, which can be solved in closed form. The distributed-parameter model of long transmission lines is considered and its parameters are estimated in a non-iterative manner using RTU measurements. The method is also extended to estimate transformer series impedance and tap position by SCADA measurements, linearly. As such, the disadvantages associated with the previous iterative approach, e.g. concern over convergence, for transmission line parameters are avoided. Moreover, the novel technique for estimating transformer parameters allows to determine the tap position as well as updated transformer series impedance. Furthermore, a thorough analysis is presented to take the measurement accuracy into account. Simulation results for different transmission lines and transformers in the IEEE 118-bus test system are reported, where the result indicate successful performance of the proposed algorithms.**

***Index Terms*—Parameter Estimation, Supervisory Control and Data Acquisition (SCADA), Transmission Line, Transmission Transformer.**

I. Nomenclature

$\boldsymbol{A}, B, \boldsymbol{C}$	Known variables for line parameter estimation.
$D, \boldsymbol{E}, \boldsymbol{F}, \boldsymbol{G}$	Known variables for transformer parameter estimation.
$\boldsymbol{Z}_c$	Surge impedance of the transmission line.
$\boldsymbol{\gamma}$	Propagation constant of the transmission line.
$\boldsymbol{z}$	Series impedance of the transformer.
τ	Tap ratio of the transformer.
V_R	Receiving-end voltage amplitude.
V_S	Sending-end voltage Amplitude.
$\boldsymbol{V}_S$	Sending-end voltage phasor with respect to V_R.
$\boldsymbol{I}_R$	Receiving-end current phasor expressed with respect to V_R.
$\boldsymbol{I}_S$	Sending-end current phasor expressed with respect to V_S.
P_S, Q_S, I_S	Sending-end measurements of active power, reactive power and current amplitude.
P_R, Q_R, I_R	Receiving-end measurements of active power, reactive power and current amplitude.
δ	Unknown synchronization angle between sending- and receiving-end voltages.
$\sigma^2_{I_R}, \sigma^2_{I_S}$	Variance of I_R and I_S measurements.
$\sigma^2_{\zeta_S}, \sigma^2_{\zeta_R}$	Variance of current angle measurements.
$\mathbf{R}$	Complex-valued covariance matrix.
$\mathbb{E}(.)$	Expected value of the argument.

A. Salehi Dobakhshari is with the Faculty of Engineering, University of Guilan, Rasht 4199613776, Iran (e-mail: salehi_ahmad@guilan.ac.ir).

V. Terzija is with the School of Electrical and Electronic Engineering, The University of Manchester, Manchester M13 9PL, U.K. (e-mail: vladimir.terzija@manchester.ac.uk).

Sadegh Azizi is with the School of Electronic and Electrical Engineering, University of Leeds, Leeds LS2 9JT, U.K. (e-mail: s.azizi@leeds.ac.uk).

II. Introduction

Accurate data plays a vital role in many aspects of power system operation and protection. In particular, transmission line parameters are essential in many applications such as setting of protective relays, optimal power flow and power system state estimation among others. In addition, the time-dependency of overhead line parameters is another subject that has attracted attention recently, for example in dynamic thermal rating [1], [2]. Likewise, there is a concern in many studies such as state estimation that the updated tap positions of transmission transformers are not communicated to the control center [3], [4]. This motivated later works on parameter error estimation based on state estimation results [4]–[8]. Other attempts included transformer parameters estimation utilizing measurements at transformer terminals [9], [10]. With the introduction of GPS-synchronized measurements, estimation of distributed-parameter model could include the measured phase-angle difference of voltages across the line into the formulation. One approach is taking possible synchronization errors into account, which results in nonlinear formulations developed in [11]–[16] based on least-squares estimation. Another approach is utilizing the phasor representation of voltage and currents, thanks to the synchronized measurements, thereby solving a linear system of equations [17]–[26].

GPS-synchronized measurements may not be available on both line terminals. Utilizing both SCADA and PMU measurements, the authors in [27] adopt an iterative approach to estimate the parameters of long transmission lines. Compared to scarce PMU measurements, SCADA measurements

TABLE I
CONTRIBUTION OF THE PROPOSED METHOD OVER PREVIOUS ALGORITHMS

Formulation \ Measurement	Synchronized	Unsynchronized
Nonlinear	[11]–[16]	[5], [6], [27], [29], [30]
Linear	[17]–[26]	Proposed Method

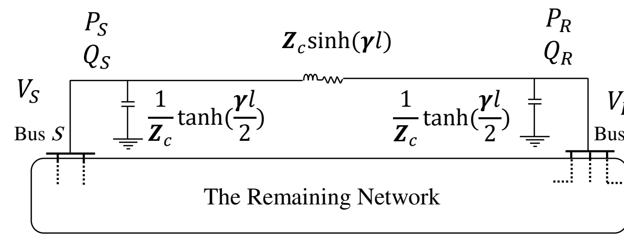

Fig. 1. Single-line-diagram of the distributed model of transmission line.

are abundant across the grid so that system operators can deploy this data with no need for additional hardware [28]. In this regard, in [29], [30] iterative methods are presented to estimate the distributed-model parameters of transmission lines, utilizing voltage, current and active and reactive power flow measurements provided by SCADA system.

The importance of the transformer parameters lies in their role in power system analysis, which is vital for many planning and operation routines in the industry. For example, state estimation in the Indian system revealed that many transformer tap positions and winding parameters have been incorrect in the database [31]. State estimation used in energy management system (EMS) needs updated tap positions of the transformers, which may not be communicated to the control center [32].

Foregoing research works either rely on synchronized measurements or resort to iteration-based methods for real-time line and transformer parameter estimation (See Table, in which the position of the new method presented in this paper is put into the context of the existing approaches). This paper presents a novel approach that utilizes SCADA measurements for estimating the accurate parameters of the distributed model of transmission lines. Utilization of SCADA measurements has the added value that the updated parameters may be integrated into existing functions in the control center, such as optimal power flow and state estimation.

The drawback of iterative methods is the need for initialization as well as the possibility of divergence of the algorithm or getting trapped in local optima, as the problem is essentially modeled as an optimization problem. For example, when the identity matrix is used as the covariance matrix for the algorithm in [27], several cases of algorithm divergence have been observed. In contrast, in this paper, a direct non iterative method is developed to give closed-form solution for series impedance and shunt admittance of the distributed parameter line model. The method proposed uses exactly the same set of SCADA measurements, i.e. bus voltage and active and reactive power flows of the line. The linear formulation is extended to estimate series impedance and tap position of transmission transformers. As such, the method has the potential to be integrated in existing EMS in control system for various applications which need updated line parameters.

III. TRANSMISSION-LINE PARAMETER ESTIMATION

Fig. 1 shows the single-line diagram of a transmission line connected to buses S and R. It is assumed that RTUs at either end of the line communicate bus voltage as well as active and reactive power and current through the line to the control center. It should be emphasized that these data are not synchronized with GPS signal. Therefore, the phase-angle difference between sending- and receiving-end voltages is unknown δ. It should be noted that we assume the system is in steady state when each set of SCADA measurements is collected so that the phase-angle difference between voltages at two line terminals is considered to be constant. Complex currents at either end of the line are calculated based on the corresponding active and reactive power measurements, as follows:

$$\boldsymbol{I}_S = I_S e^{-j\left(tg^{-1}\frac{Q_S}{P_S}\right)} \tag{1}$$

where I_S, P_S and Q_S are real-valued measurements provided by SCADA data from RTUs at substation S. If I_S is not communicated to the control center, it can be calculated by corresponding active and reactive power measurements, along with the voltage measurement, as follows.

$$I_S = \frac{\sqrt{P_S^2 + Q_S^2}}{V_S} \tag{2}$$

Similar to (1), $\boldsymbol{I}_R$ may be expressed as

$$\boldsymbol{I}_R = I_R e^{-j\left(tg^{-1}\frac{Q_R}{P_R}\right)} \tag{3}$$

And if I_R is not available, it can be calculated indirectly as

$$I_R = \frac{\sqrt{P_R^2 + Q_R^2}}{V_R} \tag{4}$$

It is worth noting at this point that regular and bold fonts correspond to real- and complex-valued variables, respectively. It should be noted that in (1) and (3) the phase of the currents at the line terminals is expressed with respect to each terminal voltage. The following equation relates sending- and receiving-end voltages and currents phasors [33]:

$$\begin{bmatrix} \boldsymbol{V}_S \\ \boldsymbol{I}_S \end{bmatrix} = \begin{bmatrix} \cosh(\boldsymbol{\gamma} l) & \boldsymbol{Z}_c \sinh(\boldsymbol{\gamma} l) \\ \frac{\sinh(\boldsymbol{\gamma} l)}{\boldsymbol{Z}_c} & \cosh(\boldsymbol{\gamma} l) \end{bmatrix} \begin{bmatrix} \boldsymbol{V}_R \\ -\boldsymbol{I}_R \end{bmatrix} \tag{5}$$

Given that local voltage and current phase-angle are known based on (1) and (3), we can rewrite (5) as follows, assuming that receiving-end voltage is the phasor reference with zero phase angle:

$$\begin{bmatrix} V_S e^{j\delta} \\ \boldsymbol{I}_S e^{j\delta} \end{bmatrix} = \begin{bmatrix} \cosh(\boldsymbol{\gamma} l) & \boldsymbol{Z}_c \sinh(\boldsymbol{\gamma} l) \\ \frac{\sinh(\boldsymbol{\gamma} l)}{\boldsymbol{Z}_c} & \cosh(\boldsymbol{\gamma} l) \end{bmatrix} \begin{bmatrix} V_R \\ -\boldsymbol{I}_R \end{bmatrix} \tag{6}$$

It is worth noting that the synchronization argument, i.e. $e^{j\delta}$, is unknown due to unsynchronized measurements at substations S and R. In (6), the phasor voltage $\boldsymbol{V}_R$ is assumed to be at an angle of $0°$, and all other voltages and currents are compared to that reference. Therefore $\boldsymbol{V}_R = V_R$. Moreover we have written $\boldsymbol{V}_S = V_S e^{j\delta}$. Therefore, in (6), V_S and V_R are real-valued while $\boldsymbol{I}_S$ and $\boldsymbol{I}_R$ are complex-valued (as they are expressed with reference to their corresponding voltage). Dividing the two equations resulting from (6) yields:

$$\frac{V_S}{\boldsymbol{I}_S} = \frac{\cosh(\boldsymbol{\gamma} l) V_R - \boldsymbol{Z}_c \sinh(\boldsymbol{\gamma} l) \boldsymbol{I}_R}{\frac{\sinh(\boldsymbol{\gamma} l)}{\boldsymbol{Z}_c} V_R - \cosh(\boldsymbol{\gamma} l) \boldsymbol{I}_R} \tag{7}$$

which may be rewritten as

$$\boldsymbol{A} \left\{ \boldsymbol{Z}_c \sinh(\boldsymbol{\gamma} l) \right\} + B \left\{ \frac{\sinh(\boldsymbol{\gamma} l)}{\boldsymbol{Z}_c} \right\} = \boldsymbol{C} \left\{ \cosh(\boldsymbol{\gamma} l) \right\} \tag{8}$$

which can be rewritten as

$$\boldsymbol{A} \left\{ \boldsymbol{Z}_c \tanh(\boldsymbol{\gamma} l) \right\} + B \left\{ \frac{\tanh(\boldsymbol{\gamma} l)}{\boldsymbol{Z}_c} \right\} = \boldsymbol{C} \tag{9}$$

where

$$\boldsymbol{A} = \boldsymbol{I}_R \boldsymbol{I}_S \tag{10}$$

$$B = V_S V_R \tag{11}$$

$$\boldsymbol{C} = V_S \boldsymbol{I}_R + V_R \boldsymbol{I}_S \tag{12}$$

where $\boldsymbol{A}$, B and $\boldsymbol{C}$ are functions of measurements, and hence known. If we have n sets of measurements ($n \geqslant 2$), an overdetermined system of equations is obtained as

$$\begin{bmatrix} \boldsymbol{A}_1 & B_1 \\ \boldsymbol{A}_2 & B_2 \\ \vdots & \vdots \\ \boldsymbol{A}_n & B_n \end{bmatrix} \begin{bmatrix} \boldsymbol{Z}_c \tanh(\boldsymbol{\gamma} l) \\ \frac{\tanh(\boldsymbol{\gamma} l)}{\boldsymbol{Z}_c} \end{bmatrix} = \begin{bmatrix} \boldsymbol{C}_1 \\ \boldsymbol{C}_2 \\ \vdots \\ \boldsymbol{C}_n \end{bmatrix} \tag{13}$$

We can solve for $\boldsymbol{Z}_c \tanh(\boldsymbol{\gamma} l)$ and $\frac{\tanh(\boldsymbol{\gamma} l)}{\boldsymbol{Z}_c}$ by the ordinary linear least-squares (OLS) method, ignoring the difference in variances of measurements, as follows.

$$\boldsymbol{Z}_c \tanh(\boldsymbol{\gamma} l) = \frac{\left(\sum_{i=1}^{n} {B_i}^2\right)\left(\sum_{i=1}^{n} \boldsymbol{A}_i^* \boldsymbol{C}_i\right) - \left(\sum_{i=1}^{n} \boldsymbol{A}_i^* B_i\right)\left(\sum_{i=1}^{n} B_i \boldsymbol{C}_i\right)}{\left(\sum_{i=1}^{n} |\boldsymbol{A}_i|^2\right)\left(\sum_{i=1}^{n} {B_i}^2\right) - \left|\sum_{i=1}^{n} \boldsymbol{A}_i^* B_i\right|^2} \tag{14}$$

$$\frac{\tanh(\boldsymbol{\gamma} l)}{\boldsymbol{Z}_c} = \frac{\left(\sum_{i=1}^{n} |\boldsymbol{A}_i|^2\right)\left(\sum_{i=1}^{n} B_i \boldsymbol{C}_i\right) - \left(\sum_{i=1}^{n} \boldsymbol{A}_i B_i\right)\left(\sum_{i=1}^{n} \boldsymbol{A}_i^* \boldsymbol{C}_i\right)}{\left(\sum_{i=1}^{n} |\boldsymbol{A}_i|^2\right)\left(\sum_{i=1}^{n} {B_i}^2\right) - \left|\sum_{i=1}^{n} \boldsymbol{A}_i^* B_i\right|^2} \tag{15}$$

where $(.)^*$ denotes conjugate transpose of the complex argument. Once (13) is solved by (14) and (15), series impedance ($\boldsymbol{Z}$) and shunt admittance of the line ($\frac{\boldsymbol{Y}}{2}$) in Fig. 1 may be obtained by

$$\boldsymbol{Z} = R_\pi + jX_\pi = \frac{\boldsymbol{Z}_c \tanh(\boldsymbol{\gamma} l)}{\sqrt{1 - \boldsymbol{Z}_c \tanh(\boldsymbol{\gamma} l) \frac{\tanh(\boldsymbol{\gamma} l)}{\boldsymbol{Z}_c}}} \tag{16}$$

$$\frac{\boldsymbol{Y}}{2} = j\frac{B_\pi}{2} = \frac{1 - \sqrt{1 - \boldsymbol{Z}_c \tanh(\boldsymbol{\gamma} l) \frac{\tanh(\boldsymbol{\gamma} l)}{\boldsymbol{Z}_c}}}{\boldsymbol{Z}_c \tanh(\boldsymbol{\gamma} l)} \tag{17}$$

IV. Transformer Parameter Estimation

Transformer series impedance and tap position are estimated linearly in this paper, using SCADA measurements at both terminals of the transformer. Fig. 2 shows the general transformer model, where $\boldsymbol{z}$, $\boldsymbol{Y}_{sh}$ and τ are unknown. Let us assume that active and reactive power as well as the voltage magnitudes at both terminals of the transformer are known. Also assume that the phase-angle difference between voltage phasors at the two terminal is unknown. Complex currents at either end of the line are calculated based on the corresponding active and reactive power measurements, similar to (1) and (3). Rewriting (6) but for Fig. 2, with the assumption of unknown synchronization argument $e^{j\delta}$, due to unsynchronized measurements at terminals S and R, we have

$$\tau \boldsymbol{I}_S e^{j\delta} + \boldsymbol{I}_R = \boldsymbol{Y}_{sh} \frac{V_s}{\tau} e^{j\delta} \tag{18}$$

$$\frac{V_s}{\tau} e^{j\delta} = V_R - \boldsymbol{z} \boldsymbol{I}_R \tag{19}$$

Dividing the two equations in (18) and (19) to cancel out $e^{j\delta}$ results in:

$$\frac{Y_{sh} \frac{V_s}{\tau} - \tau \boldsymbol{I}_S}{\frac{V_s}{\tau}} = \frac{\boldsymbol{I}_R}{V_R - \boldsymbol{z} \boldsymbol{I}_R} \tag{20}$$

which may be simplified as

$$\frac{\boldsymbol{Y}_{sh}}{\tau^2} V_S V_R - V_S \boldsymbol{I}_R \frac{1 + \boldsymbol{z} \boldsymbol{Y}_{sh}}{\tau^2} + \boldsymbol{I}_S \boldsymbol{I}_R \boldsymbol{z} = V_R \boldsymbol{I}_S \tag{21}$$

which can be rewritten as the following linear complex equation

$$D \left\{ \frac{\boldsymbol{Y}_{sh}}{\tau^2} \right\} + \boldsymbol{E} \left\{ \frac{1 + \boldsymbol{z} \boldsymbol{Y}_{sh}}{\tau^2} \right\} + \boldsymbol{F} \left\{ \boldsymbol{z} \right\} = \boldsymbol{G} \tag{22}$$

where

$$D = V_S V_R \tag{23}$$

$$\boldsymbol{E} = -V_S \boldsymbol{I}_R \tag{24}$$

$$\boldsymbol{F} = \boldsymbol{I}_S \boldsymbol{I}_R \tag{25}$$

$$\boldsymbol{G} = \boldsymbol{I}_S V_R \tag{26}$$

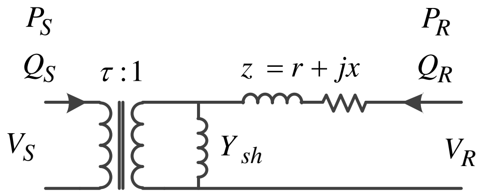

Fig. 2. Single-line-diagram of the transformer model.

It is evident that D, $\boldsymbol{E}$, $\boldsymbol{F}$ and $\boldsymbol{G}$ depend only on measurements. Similar to Section III, if we have n sets of measurements ($n \geqslant 3$) at the substation, we can form a linear system of complex equations as

$$\begin{bmatrix} D_1 & \boldsymbol{E}_1 & \boldsymbol{F}_1 \\ D_2 & \boldsymbol{E}_2 & \boldsymbol{F}_2 \\ \vdots & \vdots & \\ D_n & \boldsymbol{E}_n & \boldsymbol{F}_n \end{bmatrix} \begin{bmatrix} \frac{\boldsymbol{Y}_{sh}}{\tau^2} \\ \frac{1+\boldsymbol{z}\boldsymbol{Y}_{sh}}{\tau^2} \\ \boldsymbol{z} \end{bmatrix} = \begin{bmatrix} \boldsymbol{G}_1 \\ \boldsymbol{G}_2 \\ \vdots \\ \boldsymbol{G}_n \end{bmatrix} \tag{27}$$

which can be rewritten in compact form as

$$\mathbf{Hx} = \mathbf{y} \tag{28}$$

which is solved by OLS formulation as

$$\hat{\mathbf{x}} = (\mathbf{H}^*\mathbf{H})^{-\mathbf{1}}\mathbf{H}^*\mathbf{y} \tag{29}$$

It is straightforward to show that transformer parameters can be obtained as

$$\boldsymbol{z} = \hat{\mathbf{x}}(\mathbf{3}) \tag{30}$$

$$\boldsymbol{Y}_{sh} = \frac{\hat{\mathbf{x}}(\mathbf{1})}{\hat{\mathbf{x}}(\mathbf{2}) - \hat{\mathbf{x}}(\mathbf{1})\hat{\mathbf{x}}(\mathbf{3})} \tag{31}$$

$$\tau = \frac{1}{\sqrt{\hat{\mathbf{x}}(\mathbf{2}) - \hat{\mathbf{x}}(\mathbf{1})\hat{\mathbf{x}}(\mathbf{3})}} \tag{32}$$

It should be noted that although there are non-linear links between the estimates in $\hat{\mathbf{x}}$ and desired parameters in (30), (31) and (32), a single value for each of the three parameters in the latter equations are obtained. The only concern might be that $\hat{\mathbf{x}}(\mathbf{2}) - \hat{\mathbf{x}}(\mathbf{1})\hat{\mathbf{x}}(\mathbf{3})$ under the square root in (32) is negative. This has never happened in our simulations. However, if it occurs, the estimation result will be inconclusive, as the reason would be wrong input data. It should be noted that in this case, there are not multiple solutions.

V. Measurement Error Analysis

If the measurements were perfect, (14) and (15) could give the exact values for transmission line parameters. That is in Sections III and IV, the OLS method was utilized to estimate line and transformer parameters, regardless of accuracy class of voltage, current and active and reactive power flow meters. In this part, the weighted linear least-squares estimation is utilized to estimate line and transformer parameters considering the statistical distribution of measurement errors.

A. Complex Random Variable: Mean and Variance

In this part we provide theoretical basis for an optimal estimation of transmission line and transformer parameters. The problem we are dealing with may be expressed as follows: *Given the accuracy class of different measurements (voltage, current and active and reactive powers) how should (13) and (27) be solved?*

It should be noted that both the coefficient matrix and measurement vector, appearing respectively in the in the LHS and RHS of (13) and (27), are dependent on voltage, current and power flow measurements, which may have different variances according to the accuracy class of respective meters. Moreover, unlike familiar least-squares problems, both the coefficient matrix and measurement vector are complex-valued. These issues are tackled by following theorems.

Theorem 1. *Complex Linear Least Squares: Consider a complex linear estimation problem in the form of* $\mathbf{Hx}+\mathbf{e} = \mathbf{z}$*, where* $\mathbf{H}$ *and* $\mathbf{z}$ *are constant coefficient matrix and measurement vector respectively, and* $\mathbf{e}$ *is the measurement error vector. If the covariance matrix of measurements is given as* $\mathbf{R} = \mathbb{E}(\mathbf{ee}^*)$ *then the optimal estimate of* $\mathbf{x}$ *is given as* $\hat{\mathbf{x}} = (\mathbf{H}^*\mathbf{R}^{-\mathbf{1}}\mathbf{H})^{-\mathbf{1}}\mathbf{H}^*\mathbf{R}^{-\mathbf{1}}\mathbf{z}$ *[34].*

Note that Theorem 1 provides a different estimation compared to the OLS practiced for (13) to give (14) and (15). Theorem 1 shows how variance values of measurements should be taken into account for an optimal estimate. However, it is uncommon to define complex variances for complex measurements. The following theorem defines the complex random variable and its statistical properties.

Theorem 2. Consider $\boldsymbol{z} = re^{j\theta}$ is a complex random variable defined by two real-valued independent Gaussian random variables $r \sim \mathcal{N}(r^t, \sigma_r^2)$ and $\theta \sim \mathcal{N}(\theta^t, \sigma_\theta^2)$. If we define $\boldsymbol{z}^t = r^t e^{j\theta^t}$ and $\boldsymbol{z} = \boldsymbol{z}^t + \boldsymbol{\varepsilon}$ then $\boldsymbol{\mu}_t(\boldsymbol{z}^t) = \mathbb{E}(\boldsymbol{\varepsilon}|\boldsymbol{z}^t) = \boldsymbol{z}^t(e^{-\frac{\sigma_\theta^2}{2}} - 1)$ and $R_z^t = var(\boldsymbol{\varepsilon}|\boldsymbol{z}^t) = \mathbb{E}(|\boldsymbol{\varepsilon} - \boldsymbol{\mu}_t|^2\,|\boldsymbol{z}^t) = \sigma_r^2 + {r^t}^2(1 - e^{-\sigma_\theta^2})$.

Proof. See Appendix A.

Theorem 2 may be interpreted as the definition of a complex random variable $\boldsymbol{z}$ with complex error $\boldsymbol{\varepsilon}$. It implies that if the magnitude and phase angle of a phasor have independent Gaussian distributions, the complex phasor have non-zero complex mean and variance, whose values are dependent on the variances of the magnitude and phase angle of that phasor. Other implication of Theorem 2 is that if complex measurements are functions of complex state variables, then the estimation will be biased.

Mean and variance expressed in Theorem 2, however, cannot be directly used, as they are functions of the true values of magnitude and phase angle, which are not available in practice. Therefore, their expected value conditioned on the measured magnitude and phase angle are used.

Theorem 3. Consider complex random variable $\boldsymbol{z} = \boldsymbol{z}^t + \boldsymbol{\varepsilon}$ and a complex measurement of this RV as $\boldsymbol{z}^m = r^m e^{j\theta^m}$. Average mean and variance of $\boldsymbol{\varepsilon}$ conditioned on this measurement can be obtained as $\mu_a = \mathbb{E}(\boldsymbol{\mu}_t(\boldsymbol{z}^t)|\boldsymbol{z}^m) = \boldsymbol{z}^m(e^{-\sigma_\theta^2} - e^{-\frac{\sigma_\theta^2}{2}})$ and $R_z^a = \mathbb{E}(R_z^t|\boldsymbol{z}^m) = \sigma_r^2(2 - e^{-\sigma_\theta^2}) + r^{m2}(1 - e^{-\sigma_\theta^2})$, respectively.

Proof. See Appendix B.

It is worth noting that Theorems 2 and 3 could have been developed from [35], which uses real-valued RVs. However, by Theorems 2 and 3 and their proofs here we have avoided Cartesian coordinates that result in much more complicated formulations. In addition, Theorem 1 is utilized in order to utilize the complex measurements, directly.

Another point is that similar to [21], [26] and other research works on transmission line parameter estimation, we assume that ratio error and phase-displacement error of instrument transformers are independent. This has also been verified experimentally in [36] where magnitude and angle measurements are treated as independent Gaussian random variables. Consider the following system of complex linear equations with ($n \geqslant p$):

$$\begin{bmatrix} \boldsymbol{H}_{11} & ... & \boldsymbol{H}_{1p} \\ \vdots & \ddots & \vdots \\ \boldsymbol{H}_{n1} & ... & \boldsymbol{H}_{np} \end{bmatrix} \begin{bmatrix} \boldsymbol{x}_1 \\ \vdots \\ \boldsymbol{x}_p \end{bmatrix} = \begin{bmatrix} \boldsymbol{z}_1^t \\ \vdots \\ \boldsymbol{z}_n^t \end{bmatrix} \tag{33}$$

If we have complex measurements whose magnitude and phase angle follow Gaussian distributions, independently, we can rewrite (33) as

$$\begin{bmatrix} \boldsymbol{H}_{11} & ... & \boldsymbol{H}_{1p} \\ \vdots & \ddots & \vdots \\ \boldsymbol{H}_{n1} & ... & \boldsymbol{H}_{np} \end{bmatrix} \begin{bmatrix} \boldsymbol{x}_1 \\ \vdots \\ \boldsymbol{x}_p \end{bmatrix} + \begin{bmatrix} \varepsilon_1 \\ \vdots \\ \varepsilon_n \end{bmatrix} = \begin{bmatrix} \boldsymbol{z}_1^m \\ \vdots \\ \boldsymbol{z}_n^m \end{bmatrix} \tag{34}$$

If we define $\bar{\boldsymbol{z}}_i = \boldsymbol{z}_i^m - \boldsymbol{z}_i^m(e^{-\sigma_\theta^2} - e^{-\frac{\sigma_\theta^2}{2}})$, then we can obtain the weighted least-squares error estimation of $\mathbf{x}$ based on Theorem 1 as follows.

$$\hat{\mathbf{x}} = (\mathbf{H}^*\mathbf{R}^{-1}\mathbf{H})^{-1}\mathbf{H}^*\mathbf{R}^{-1}\bar{\mathbf{z}} \tag{35}$$

where based on the independence of n measurement sets, $\mathbf{R}$ is the diagonal covariance matrix whose elements are given according to Theorem 3. It should be noted that it has been implicitly assumed in (35) that $\mathbf{H}^*\mathbf{R}^{-1}\mathbf{H}$ is non-singular. Therefore, similar measurements cannot be used in the proposed method and similar to previous literature, multi-scan measurements [11], [27], [29] are used.

Lemma 1. If $\mathbf{y} = \boldsymbol{f}(\hat{\mathbf{x}})$ where $\hat{\mathbf{x}}$ is given in (35) and $\boldsymbol{f} : \mathbb{C}^p \to \mathbb{C}^q$ is a given nonlinear function, then:

$$Cov(\mathbf{y}) = \mathbf{J}^* Cov(\hat{\mathbf{x}})\mathbf{J} \tag{36}$$

where $\mathbf{J}$ is the Jacobian matrix of $\boldsymbol{f}$ and $Cov(\hat{\mathbf{x}}) = (\mathbf{H}^*\mathbf{R}^{-1}\mathbf{H})^{-1}$ [37].

Lemma 1 helps us find the covariance of the transmission and transformer parameter estimates.

B. Weighted Linear Least-Squares Estimation of Transmission Line Parameters

We aim to write (13) in the form of (34). It should be noted that $\boldsymbol{A}$, B and $\boldsymbol{C}$ are functions of measurements. Therefore, there are deviations between their true and measured values. For example we have

$$\boldsymbol{A}^{meas} = \boldsymbol{A}^{true} + \boldsymbol{\varepsilon}_A \tag{37}$$

where $\boldsymbol{A}^{true}$ is a function of true yet unknown values of $\boldsymbol{I}_S$ and $\boldsymbol{I}_R$ according to (10) and $\boldsymbol{\varepsilon}_A$ is given in Appendix C. This also holds for B and $\boldsymbol{C}$. As such, (13) may be expanded as

$$\begin{bmatrix} \boldsymbol{A}_1^{true} & B_1^{true} \\ \boldsymbol{A}_2^{true} & B_2^{true} \\ \vdots & \vdots \\ \boldsymbol{A}_n^{true} & B_n^{true} \end{bmatrix} \begin{bmatrix} \boldsymbol{x}_1 \\ \boldsymbol{x}_2 \end{bmatrix} = \begin{bmatrix} \boldsymbol{C}_1^{true} \\ \boldsymbol{C}_2^{true} \\ \vdots \\ \boldsymbol{C}_n^{true} \end{bmatrix} \tag{38}$$

which may be rewritten as

$$\begin{bmatrix} \boldsymbol{A}_1^{meas} & B_1^{meas} \\ \boldsymbol{A}_2^{meas} & B_2^{meas} \\ \vdots & \vdots \\ \boldsymbol{A}_n^{meas} & B_n^{meas} \end{bmatrix} \begin{bmatrix} \boldsymbol{x}_1 \\ \boldsymbol{x}_2 \end{bmatrix} = \begin{bmatrix} \boldsymbol{C}_1^{meas} + \boldsymbol{\varepsilon}_{\boldsymbol{A}_1}\boldsymbol{x}_1 + \varepsilon_{B_1}\boldsymbol{x}_2 - \boldsymbol{\varepsilon}_{\boldsymbol{C}_1} \\ \boldsymbol{C}_2^{meas} + \boldsymbol{\varepsilon}_{\boldsymbol{A}_2}\boldsymbol{x}_1 + \varepsilon_{B_2}\boldsymbol{x}_2 - \boldsymbol{\varepsilon}_{\boldsymbol{C}_2} \\ \vdots \\ \boldsymbol{C}_n^{meas} + \boldsymbol{\varepsilon}_{\boldsymbol{A}_n}\boldsymbol{x}_1 + \varepsilon_{B_n}\boldsymbol{x}_2 - \boldsymbol{\varepsilon}_{\boldsymbol{C}_n} \end{bmatrix} \tag{39}$$

which may be rewritten in standard form as

$$\begin{bmatrix} \boldsymbol{A}_1^{meas} & B_1^{meas} \\ \boldsymbol{A}_2^{meas} & B_2^{meas} \\ \vdots & \vdots \\ \boldsymbol{A}_n^{meas} & B_n^{meas} \end{bmatrix} \begin{bmatrix} \boldsymbol{x}_1 \\ \boldsymbol{x}_2 \end{bmatrix} + \begin{bmatrix} \varepsilon_1 \\ \varepsilon_2 \\ \vdots \\ \varepsilon_n \end{bmatrix} = \begin{bmatrix} \boldsymbol{C}_1^{meas} \\ \boldsymbol{C}_2^{meas} \\ \vdots \\ \boldsymbol{C}_n^{meas} \end{bmatrix} \tag{40}$$

where $\boldsymbol{x}_1$ and $\boldsymbol{x}_2$ denote respectively $\boldsymbol{Z}_c \tanh(\boldsymbol{\gamma} l)$ and $\dfrac{\tanh(\boldsymbol{\gamma} l)}{\boldsymbol{Z}_c}$, and ε_i is the cumulative measurement error in this linear formulation, whose expected value and variance can be found in terms of the true value and variance of related measurements. If (40) is rewritten in the form of $\mathbf{Hx} + \boldsymbol{\varepsilon} = \mathbf{z}$ then, according to Theorem 3, elements of diagonal covariance matrix $\mathbf{R} = \mathbb{E}(\boldsymbol{\varepsilon}\boldsymbol{\varepsilon}^*) - |\mathbb{E}(\boldsymbol{\varepsilon})|^2$ can be found by

$$\mathbb{E}(\varepsilon_i\varepsilon_i^*) = \mathbb{E}((\boldsymbol{\varepsilon}_{\boldsymbol{C}_i} - \boldsymbol{\varepsilon}_{\boldsymbol{A}_i}\boldsymbol{x}_1 - \varepsilon_{B_i}\boldsymbol{x}_2)(\boldsymbol{\varepsilon}_{\boldsymbol{C}_i} - \boldsymbol{\varepsilon}_{\boldsymbol{A}_i}\boldsymbol{x}_1 - \varepsilon_{B_i}\boldsymbol{x}_2)^*) \tag{41}$$

which can be extended as

$$\begin{aligned} \mathbb{E}(\varepsilon_i\varepsilon_i^*) = \mathbb{E}(\{&\boldsymbol{\varepsilon}_{\boldsymbol{C}_i}\boldsymbol{\varepsilon}_{\boldsymbol{C}_i}^* + \boldsymbol{\varepsilon}_{\boldsymbol{A}_i}\boldsymbol{\varepsilon}_{\boldsymbol{A}_i}^*|\boldsymbol{x}_1|^2 + \varepsilon_{B_i}\varepsilon_{B_i}^*|\boldsymbol{x}_2|^2 \\ &-\boldsymbol{\varepsilon}_{\boldsymbol{A}_i}\boldsymbol{\varepsilon}_{\boldsymbol{C}_i}^*\boldsymbol{x}_1 - \varepsilon_{B_i}\boldsymbol{\varepsilon}_{\boldsymbol{C}_i}^*\boldsymbol{x}_2 - \boldsymbol{\varepsilon}_{\boldsymbol{C}_i}\boldsymbol{\varepsilon}_{\boldsymbol{A}_i}^*\boldsymbol{x}_1^* - \boldsymbol{\varepsilon}_{\boldsymbol{C}_i}\varepsilon_{B_i}^*\boldsymbol{x}_2^*\}) \end{aligned} \tag{42}$$

where the expected value of each term is detailed in Appendix C. It should be noted that $\boldsymbol{A}_i$ and B_i are independent according to (10) and (11), and therefore the bilinear terms involving them have been dropped. To obtain the bias of the estimation error, it is sufficient to expand $\mathbb{E}(\varepsilon_i)$ as

$$\begin{aligned} \mathbb{E}(\varepsilon_i) &= \mathbb{E}(\boldsymbol{\varepsilon}_{\boldsymbol{C}_i} - \boldsymbol{\varepsilon}_{\boldsymbol{A}_i}\boldsymbol{x}_1 - \varepsilon_{B_i}\boldsymbol{x}_2) \\ &= \mathbb{E}(\boldsymbol{\varepsilon}_{\boldsymbol{C}_i}) - \boldsymbol{x}_1^{true}\mathbb{E}(\boldsymbol{\varepsilon}_{\boldsymbol{A}_i}) - \boldsymbol{x}_2^{true}\mathbb{E}(\varepsilon_{B_i}) \end{aligned} \tag{43}$$

where $\mathbb{E}(\boldsymbol{\varepsilon}_{\boldsymbol{A}_i})$, $\mathbb{E}(\varepsilon_{B_i})$ and $\mathbb{E}(\boldsymbol{\varepsilon}_{\boldsymbol{C}_i})$ are detailed in Appendix C. It should be noted that the elements of the covariance matrix obtained by (42) and (43) are also functions of state variables. OLS gives a good approximation of state variables in this regard and therefore $\boldsymbol{x}_1^t$ and $\boldsymbol{x}_2^t$ are approximated by (14) and (15), respectively.

Transmission line parameters can be obtained from $\boldsymbol{x}_1$ and $\boldsymbol{x}_2$ by (16) and (17). Therefore, Lemma 1 can be used to obtain the variance of the estimated series impedance and shunt admittance of the line. From (16) and (17), the non-linear function $\boldsymbol{f}$ in Lemma 1 is as follows:

$$\boldsymbol{f} = \begin{bmatrix} \dfrac{\boldsymbol{x}_1}{\sqrt{1-\boldsymbol{x}_1\boldsymbol{x}_2}} \\ \\ \dfrac{1-\sqrt{1-\boldsymbol{x}_1\boldsymbol{x}_2}}{\boldsymbol{x}_1} \end{bmatrix} \quad (44)$$

VI. Simulation Results

To evaluate the proposed algorithms, IEEE 118-bus test system is utilized for transmission line and transformer parameter estimation. Seven snapshots of the system are simulated by varying load, generation and voltage set-points of generator buses. Active and reactive power as well as current and voltage at either end of the line, simulating RTU measurements at different operating conditions, are then input into MATLAB, where the estimation algorithm is implemented.

A. Transmission Lines

A long 345-kV line in the IEEE 118-bus test network, connecting buses 38 and 65, is simulated in DIgSILENT and studied here. The errors of voltage and current measurements depend on the accuracy class of the corresponding measurements. Class 0.5 instrument transformers are assumed to provide input measurements to the proposed algorithm [38]. Based on the maximum allowable error for this class in IEC standards [39], [40], a Gaussian error is attributed to each instrument transformer as in [26]. The measurement error can be a function of the measurand if the measured value is much less than the rated primary quantity of the instrument transformer. For example, in [38] the variance of the measurement is expressed as a function of the measurand. Unfortunately, the measurement error distribution is not given in IEC 60819 standard. Therefore, we have followed the same methodology as in [26] and assumed a normal distribution for measurement errors which do not exceed their upper bound in 99.8% of cases. However, if the relationship between measurement error and the measurand is known explicitly, e.g. from the manufacturer's data, it can be used to define specific standard deviations for different measurements.

For each snapshot, a number of 1000 simulation cases has been carried out, where the measurements taken from the software simulator has been polluted with Gaussian zero-mean noise. Table II reports the actual surge impedance and propagation constant of this line. The series impedance and shunt susceptance of the distributed parameter-model of this line can be calculated from the foregoing parameters and are reported in the same table. The estimated line parameters are reported in Table II and can be compared with the actual line parameters.

TABLE II
Parameter Estimation for Line 38-65 in IEEE 118-bus System

Parameter	Actual Value	Mean of Estimated Value
$\boldsymbol{Z}_c(\Omega)$	$365.86 - j16.709$	$365.65 - j16.747$
$\boldsymbol{\gamma} l$	$0.014658 + j0.32148$	$0.014318 + j0.32144$
$R_\pi(\Omega)$	10.358	10.259
$X_\pi(\Omega)$	115.37	115.304
$B_\pi(\Omega^{-1})$	886.44e-6	886.67e-6

TABLE III
Parameter Estimation for 345-KV Transmission Lines in IEEE 118-bus System

Algorithm	Proposed			[27]		
Transmission Line	$\hat{R}_\pi$ Er.(%)	$\hat{X}_\pi$ Er.(%)	$\hat{B}_\pi$ Er.(%)	$\hat{R}_\pi$ Er.(%)	$\hat{X}_\pi$ Er.(%)	$\hat{B}_\pi$ Er.(%)
8-9	1.66	0.27	0.07	-0.37	0.31	0.19
9-10	0.87	-0.03	-0.05	0.50	0.10	-0.11
8-30	3.88	0.51	-0.01	10.66	-1.20	-0.05
26-30	-0.67	-0.15	-0.08	-0.10	-0.24	0.10
30-38	-2.87	0.75	0.03	4.06	-1.05	-0.02
38-65	0.74	-0.01	0.008	-2.02	0.45	-0.17
64-65	0.40	0.23	0.03	-0.86	-0.07	-0.02

TABLE IV
Parameter Estimation Uncertainties for 345-KV Transmission Lines in IEEE 118-bus System

Transmission Line	Standard deviation of $\boldsymbol{Z}_\pi$ (%)	Standard deviation of $\boldsymbol{Y}_\pi$ (%)
8-9	0.18	0.13
9-10	0.18	0.12
8-30	0.71	0.09
26-30	0.12	0.099
30-38	0.54	0.06
38-65	0.098	0.06
64-65	0.37	0.15

Table III compares the estimation errors between the proposed algorithm and the algorithm in [27] for long 345-KV transmission lines in the IEEE 118-bus test network. Class 0.5 instrument transformers are assumed to provide voltage and current measurements. For the same set of measurements, the two algorithms are implemented in MATLAB to estimate parameters of the lines. The estimation error reflected in Table III is defined as

$$Er.(\%) = \frac{True\ \ Parameter - Est.\ \ Parameter}{True\ \ Parameter} \times 100 \quad (45)$$

It should be noted that the right approach to develop the covariance matrix for [27] is obscure. The reason is that the equation used are not in the standard format of $z = f(x) + e, Cov(e) = R$. Instead, phasor measurements are included in the nonlinear function f. Unfortunately, there is no discussion in [27] regarding this aspect of the nonlinear algorithm used.

Table IV provides variance of estimates for transmission

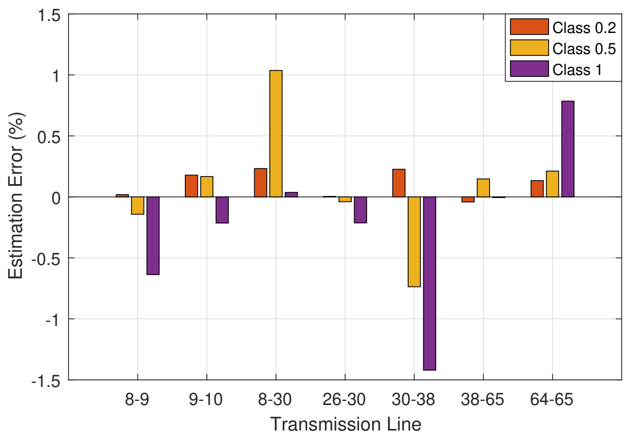

Fig. 3. Estimation results for transmission line reactances for different measurement accuracy classes.

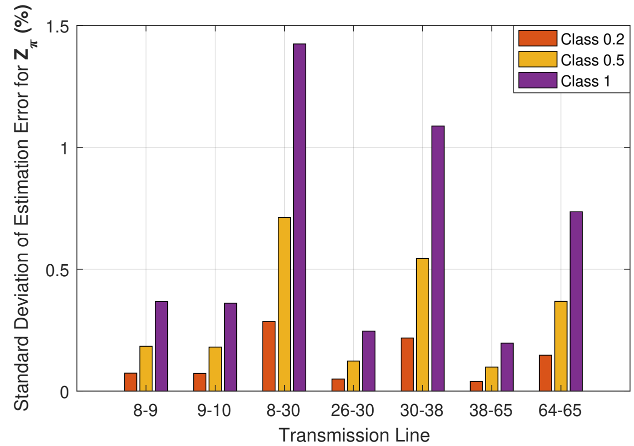

Fig. 4. Uncertainty of series impedance estimates for different measurement accuracy classes.

parameter estimation. Standard deviation of $\boldsymbol{Z}_\pi$ (and similarly $\boldsymbol{Y}_\pi$) is defined as:

$$\sigma_Z^{\%} = \frac{var(\boldsymbol{Z})}{\mid \boldsymbol{Z}^t \mid} \times 100 \tag{46}$$

where $\boldsymbol{Z}^t$ is the true impedance of the line and $var(\boldsymbol{Z})$ is obtained as follows:

$$var(\boldsymbol{Z}) = \boldsymbol{J}^*(\mathbf{H}^*\mathbf{R}^{-1}\mathbf{H})^{-1}\boldsymbol{J} \tag{47}$$

where $J = [\frac{\partial f_1}{x_1}\frac{\partial f_1}{x_2}]^T$ is the Jacobian of function f_1 given in (44), according to Lemma 1. It should be noted that although, for example for line 8-9, series resistance of the line has an error greater than 1%, the overall impedance is not changed as the standard deviation of estimate for this line is less than 0.2%. It can be seen that the proposed algorithm outperforms previous iterative algorithm in [27]. It is worth noting that the algorithm in [27] is more demanding as it needs one end of the line to be equipped with a PMU. However, GPS-synchronized measurements are not required in neither end of the line in the proposed algorithm. To study the impact of quality of measurements on the estimation error values, four sets of instrument transformers with accuracy classes of 0.2, 0.5 and 1 are employed, separately. The estimation results given in Fig. 3 for line reactance reveals that better measurements lead to more accurate estimated parameters. The standard deviations of estimates for the same lines are reflected in Fig. 4. As expected, the uncertainty of estimates increases as less accurate measurements are used. It is worth noting that in contrast to the estimates obtained in Table III and Fig. 3, which report different figures for different measurement sets, uncertainty of measurements in Fig. 4 shows a consistent behavior for each line and is also compatible with results obtained in Table IV.

B. Transformers

Several transmission transformers connecting 138- and 345-kV voltage levels in the IEEE 118-bus test network are examined. Estimation of transformer parameters is also based on weighted least-squares approach developed in Section V. However, to save space, the details of the derivations are not included. The actual values of transformer tap and impedance used in simulations are given in Table V. It is worth noting that the tap position is a discrete unknown value in practice, although the estimation process gives a continuous value. This may be useful to identify the tap position which results in closest τ for the transformer model. Moreover, τ is real-valued though (32) gives a complex value. Therefore we have used the real part of (32) in Table VI. In addition, it is assumed that the vector group of the transformer is available. Five snapshots of the system are taken from the software simulator and 1000 random cases considering the measurement errors are simulated for each snapshot.

TABLE V
Actual Parameters of Transformers in IEEE 118-bus System

Transformer	$\boldsymbol{z}$ (pu)	τ	$\boldsymbol{Y}_{sh}(pu)$
8-5	$j0.0267$	0.985	$j0.015$
26-25	$j0.0382$	0.96	$j0.015$
30-17	$j0.0388$	0.96	$j0.015$
38-37	$j0.0375$	0.935	$j0.015$
63-59	$j0.0386$	0.96	$j0.015$

TABLE VI
Parameter Estimation for Different Transformers

Trf	Ignoring Y_{sh}		Considering Y_{sh}		
	$z(\%)$	τ	z $(\%)$	τ	$Y_{sh}(\%)$
8-5	2.6099	0.9842	2.6687	0.9859	1.61
26-25	2.7601	0.9575	3.7806	0.9612	1.54
30-17	3.7563	0.9589	3.8777	0.9608	1.59
38-37	3.6421	0.9339	3.7529	0.9358	1.55
63-59	3.5963	0.9842	3.8261	0.9614	1.54

All transformers are considered to have 1.5% no-load current. In order to assess the importance of modeling the shunt branch of the transformer, two sets of estimations have been carried out, whose results are shown in Table VI. First, the shunt branch is ignored. Therefore, $\boldsymbol{Y}_{sh}$ in (22) will be zero and a similar procedure is followed to find $\boldsymbol{z}$ and τ. Second, $\boldsymbol{Y}_{sh}$ is considered in the equations. It should be noted that τ is a discrete variable while the estimated tap values reflected in Table VI are the continuous estimated values. The tap position is decided based on these estimates. For example if each tap position changes the voltage by 1% then for transformer 63-59, τ is estimated 0.98 when ignoring the shunt branch and 0.96 when considering it. According to Table V, in order to correctly estimate the tap position, the shunt branch has to be considered. Moreover, if estimated series branches for the two formulations are compared, one can verify from Tables V and VI that taking the shunt branch into account increases the accuracy of estimates considerably.

VII. Conclusion

A novel linear formulation has been presented in this paper to estimate transmission-line and transformer parameters by unsynchronized SCADA measurements. A thorough statistical analysis has been carried out to take different variance values of measurements into account. The output of the estimation process is useful in many applications including power system operation, state estimation, planning and protection. In particular, online procedures in power system operation and adaptive protection may employ the method as an additional function for updating their input parameters or detect measurement errors. Simulation results for the IEEE 118-bus test system revealed successful estimation of line parameters as well as transformer series impedance and tap position. Compared to a previous iterative algorithm, the proposed algorithm in general yields more accurate results, without the concern over convergence of the algorithm. Simulation results show the importance of the accuracy class of instrument transformers for the proposed algorithm. Accurate measurements yield accurate estimation results for parameters of transmission lines and transformers. Using class 0.5 measurements in the proposed algorithms results in parameter estimation errors less than 1% in most cases.

Appendix A
Proof of Theorem 2

Consider a complex random variable $=re^{j\theta}$ defined by two real-valued random variables $r\sim\mathcal{N}(r^t,\sigma_r^2)$ and $\theta\sim\mathcal{N}(\theta^t,\sigma_\theta^2)$, which are independent. Therefore $\boldsymbol{z}$ can be written as

$$re^{j\theta} = (r^t+\varepsilon_r)e^{j(\theta^t+\varepsilon_\theta)} \tag{A.1}$$

where $\varepsilon_r \sim \mathcal{N}(0,\sigma_r^2)$ and $\varepsilon_\theta \sim \mathcal{N}(0,\sigma_\theta^2)$ are independent measurement errors of magnitude and phase-angle of $\boldsymbol{z}$, respectively. Rewriting (A.1) in terms of true value of the complex random variable and its error we have

$$re^{j\theta} = r^t e^{j\theta^t} + \boldsymbol{\varepsilon} \tag{A.2}$$

where the complex error $\boldsymbol{\varepsilon}$ is given by

$$\begin{aligned}\boldsymbol{\varepsilon} &= (r^t+\varepsilon_r)e^{j(\theta^t+\,\varepsilon_\theta)} - r^t e^{j\theta^t}\\ &= r^t(e^{j(\theta^t+\,\varepsilon_\theta)} - e^{j\theta^t}) + \varepsilon_r e^{j(\theta_t+\,\varepsilon_\theta)}\\ &= r^t e^{j\theta^t}(e^{j\varepsilon_\theta}-1) + \varepsilon_r e^{j(\theta_t+\,\varepsilon_\theta)}\\ &= \boldsymbol{z}^t(e^{j\varepsilon_\theta}-1) + \varepsilon_r e^{j(\theta_t+\,\varepsilon_\theta)}\end{aligned} \tag{A.3}$$

On the one hand, ε_r is independent of ε_θ and any function of it so that the expected value of the second term in the last line of (A.3) is zero. On the other hand for the Gaussian random variable ε_θ we have [41]

$$\mathbb{E}(e^{-j\varepsilon_\theta}) = \mathbb{E}(e^{j\varepsilon_\theta}) = e^{-\frac{{\sigma_\theta}^2}{2}} \tag{A.4}$$

which, provided that $\mathbb{E}(\varepsilon_r)=0$, yields

$$\boldsymbol{\mu}_t(\boldsymbol{z}^t) = \mathbb{E}(\boldsymbol{\varepsilon}|\boldsymbol{z}^t) = \boldsymbol{z}^t(e^{-\frac{\sigma_\theta^2}{2}}-1) \tag{A.5}$$

To obtain variance of $\boldsymbol{\varepsilon}$ conditioned on $\boldsymbol{z}^t$, using the last line of (A.3) as well as (A.5) we can write:

$$\begin{aligned}&var(\boldsymbol{\varepsilon}) = \mathbb{E}(|\boldsymbol{\varepsilon}-\mathbb{E}(\boldsymbol{\varepsilon})|^2)\\ &= \mathbb{E}(|\boldsymbol{z}^t(e^{j\varepsilon_\theta}-1) + \varepsilon_r e^{j(\theta_t+\,\varepsilon_\theta)} - \boldsymbol{z}^t(e^{-\frac{\sigma_\theta^2}{2}}-1)|^2)\\ &= \mathbb{E}([\boldsymbol{z}^t(e^{j\varepsilon_\theta}-e^{-\frac{\sigma_\theta^2}{2}}) + \varepsilon_r e^{j(\theta_t+\varepsilon_\theta)}]\\ &\qquad [\boldsymbol{z}^t(e^{j\varepsilon_\theta}-e^{-\frac{\sigma_\theta^2}{2}}) + \varepsilon_r e^{j(\theta_t+\varepsilon_\theta)}]^*)\\ &= {r^t}^2(1+e^{-\sigma_\theta^2} - e^{-\frac{\sigma_\theta^2}{2}}\mathbb{E}(e^{j\varepsilon_\theta}+e^{-j\varepsilon_\theta})) + \sigma_r^2\end{aligned} \tag{A.6}$$

which can be simplified using (A.4) as:

$$R_z^t = var(\boldsymbol{\varepsilon}|\boldsymbol{z}^t) = {r^t}^2(1-e^{-\sigma^2}) + \sigma_r^2 \tag{A.7}$$

Appendix B
Proof of Theorem 3

First we obtain $\mathbb{E}(\boldsymbol{\mu}_t(\boldsymbol{z}^t)|\boldsymbol{z}^m)$ using (A.5).

$$\mathbb{E}(\boldsymbol{\mu}_t(\boldsymbol{z}^t)|\boldsymbol{z}^m) = \mathbb{E}((r^m-\varepsilon_r)e^{j(\theta_m-\varepsilon_\theta)}(e^{-\frac{\sigma_\theta^2}{2}}-1)) \tag{B.1}$$

As ε_r is independent of ε_θ and its functions, (C.1) can be simplified as

$$\mathbb{E}(\boldsymbol{\mu}_t(\boldsymbol{z}^t)|\boldsymbol{z}^m) = r^m e^{j\theta_m}(e^{-\frac{\sigma_\theta^2}{2}}-1)\mathbb{E}(e^{-j\varepsilon_\theta}) \tag{B.2}$$

which can be simplified using (A.4) as:

$$\mathbb{E}(\boldsymbol{\mu}_t(\boldsymbol{z}^t)|\boldsymbol{z}^m) = \boldsymbol{z}^m(e^{-\sigma_\theta^2} - e^{-\frac{\sigma_\theta^2}{2}}) \tag{B.3}$$

Now we calculate $\mathbb{E}(R_z^t|\boldsymbol{z}^m)$ using (A.7) as:

$$\mathbb{E}(R_z^t|\boldsymbol{z}^m) = \mathbb{E}([(r^m-\varepsilon_r)^2(1-e^{-\sigma^2}) + \sigma_r^2]) \tag{B.4}$$

which can be simplified as

$$\begin{aligned}\mathbb{E}(R_z^t|\boldsymbol{z}^m) &= \sigma_r^2 + {r^m}^2(1-e^{-\sigma^2})\mathbb{E}(\varepsilon_r^2)(1-e^{-\sigma^2})\\ &= \sigma_r^2(2-e^{-\sigma_\theta^2}) + {r^m}^2(1-e^{-\sigma_\theta^2})\end{aligned} \tag{B.5}$$

Appendix C
Detailed Terms in (42) and (43)

To obtain $\mathbb{E}(\boldsymbol{\varepsilon}_{\boldsymbol{A}_i})$, $\mathbb{E}(\varepsilon_{B_i})$ and $\mathbb{E}(\boldsymbol{\varepsilon}_{\boldsymbol{C}_i})$, it is required to extend each in terms of the measurements, taking measurement errors into account. We illustrate the procedure for $\mathbb{E}(\boldsymbol{\varepsilon}_{\boldsymbol{A}_i})$ as follows.

$$\begin{aligned}\boldsymbol{A}_i^{true} &= \boldsymbol{I}_{S_i}^{true}\boldsymbol{I}_{R_i}^{true} = (\boldsymbol{I}_{S_i}^{meas} - \boldsymbol{\varepsilon}_{\boldsymbol{I}_{S_i}})(\boldsymbol{I}_{R_i}^{meas} - \boldsymbol{\varepsilon}_{\boldsymbol{I}_{R_i}}) \\ &= \boldsymbol{I}_{S_i}^{meas}\boldsymbol{I}_{R_i}^{meas} - \boldsymbol{\varepsilon}_{\boldsymbol{I}_{S_i}}\boldsymbol{I}_{R_i}^{meas} - \boldsymbol{\varepsilon}_{\boldsymbol{I}_{R_i}}\boldsymbol{I}_{S_i}^{meas}\end{aligned} \tag{C.1}$$

On the other hand from (10) we have

$$\boldsymbol{A}_i^{meas} = \boldsymbol{I}_{S_i}^{meas}\boldsymbol{I}_{R_i}^{meas} \tag{C.2}$$

Substituting (C.1) and (C.2) into (37) results in

$$\boldsymbol{\varepsilon}_{\boldsymbol{A}_i} = \boldsymbol{\varepsilon}_{\boldsymbol{I}_{S_i}}\boldsymbol{I}_{R_i}^{meas} + \boldsymbol{\varepsilon}_{\boldsymbol{I}_{R_i}}\boldsymbol{I}_{S_i}^{meas} \tag{C.3}$$

Getting the expected value from both sides leads to

$$\begin{aligned}\mathbb{E}(\boldsymbol{\varepsilon}_{\boldsymbol{A}_i}) &= \boldsymbol{I}_{R_i}^{meas}\mathbb{E}(\boldsymbol{\varepsilon}_{\boldsymbol{I}_{S_i}}) + \boldsymbol{I}_{S_i}^{meas}\mathbb{E}(\boldsymbol{\varepsilon}_{\boldsymbol{I}_{R_i}}) \\ &= \boldsymbol{I}_{R_i}^{meas}\boldsymbol{I}_{S_i}^{meas}(e^{-\sigma^2_{\theta_{I_S}}} + e^{-\sigma^2_{\theta_{I_R}}} - e^{-\frac{\sigma^2_{\theta_{I_S}}}{2}} - e^{-\frac{\sigma^2_{\theta_{I_R}}}{2}})\end{aligned} \tag{C.4}$$

where the last equity is resulted from Theorem 3 provided that $\sigma^2_{\theta_{I_S}}$ and $\sigma^2_{\theta_{I_R}}$ are the variances of current phase angles at sending- and receiving-ends, respectively. A similar procedure may be followed to have

$$\mathbb{E}(\boldsymbol{\varepsilon}_{B_i}) = 0 \tag{C.5}$$

$$\begin{aligned}\mathbb{E}(\boldsymbol{\varepsilon}_{\boldsymbol{C}_i}) = & V_{S_i}^{meas}\boldsymbol{I}_{R_i}^{meas}(e^{-\sigma^2_{\theta_{I_R}}} - e^{-\frac{\sigma^2_{\theta_{I_R}}}{2}}) \\ & + V_{R_i}^{meas}\boldsymbol{I}_{S_i}^{meas}(e^{-\sigma^2_{\theta_{I_S}}} - e^{-\frac{\sigma^2_{\theta_{I_S}}}{2}})\end{aligned} \tag{C.6}$$

The elements of covariance matrix are calculated based on (42), where it is sufficient to calculate the expected value of each term and finally add them up. For example, $\mathbb{E}(\boldsymbol{\varepsilon}_{\boldsymbol{A}_i}\boldsymbol{\varepsilon}^*_{\boldsymbol{A}_i})$ can be extended based on (C.3) as

$$\mathbb{E}(\boldsymbol{\varepsilon}_{\boldsymbol{A}_i}\boldsymbol{\varepsilon}^*_{\boldsymbol{A}_i}) = I_{R_i}^{meas2}\mathbb{E}(\boldsymbol{\varepsilon}_{\boldsymbol{I}_{S_i}}\boldsymbol{\varepsilon}_{\boldsymbol{I}^*_{S_i}}) + I_{S_i}^{meas2}\mathbb{E}(\boldsymbol{\varepsilon}_{\boldsymbol{I}_{R_i}}\boldsymbol{\varepsilon}_{\boldsymbol{I}^*_{R_i}}) \tag{C.7}$$

which can be written according to Theorem 3 as

$$\begin{aligned}\mathbb{E}(\boldsymbol{\varepsilon}_{\boldsymbol{A}_i}\boldsymbol{\varepsilon}^*_{\boldsymbol{A}_i}) = & I_{R_i}^{meas2}[\sigma^2_{I_S}(2 - e^{-\sigma^2_{\theta_{I_S}}}) + I_{S_i}^{meas2}(1 - e^{-\sigma^2_{\theta_{I_S}}})] \\ & + I_{S_i}^{meas2}[\sigma^2_{I_R}(2 - e^{-\sigma^2_{\theta_{I_R}}}) + I_{R_i}^{meas2}(1 - e^{-\sigma^2_{\theta_{I_R}}})]\end{aligned} \tag{C.8}$$

A similar procedure is followed to obtain other terms in (42) as

$$\mathbb{E}(\boldsymbol{\varepsilon}_{B_i}\boldsymbol{\varepsilon}^*_{B_i}) = V_{S_i}^{meas2}\sigma^2_{V_R} + V_{R_i}^{meas2}\sigma^2_{V_S} \tag{C.9}$$

$$\begin{aligned}&\mathbb{E}(\boldsymbol{\varepsilon}_{\boldsymbol{C}_i}\boldsymbol{\varepsilon}^*_{\boldsymbol{C}_i}) = \\ &I_{R_i}^{meas2}\sigma^2_{V_S} + V_{S_i}^{meas2}[\sigma^2_{I_R}(2 - e^{-\sigma^2_{\theta_{I_R}}}) + I_{R_i}^{meas2}(1 - e^{-\sigma^2_{\theta_{I_R}}})] \\ &+ I_{S_i}^{meas2}\sigma^2_{V_R} + V_{R_i}^{meas2}[\sigma^2_{I_S}(2 - e^{-\sigma^2_{\theta_{I_S}}}) + I_{S_i}^{meas2}(1 - e^{-\sigma^2_{\theta_{I_S}}})]\end{aligned} \tag{C.10}$$

It should be noted that terminals R and S are comprised of independent measurements.

$$\begin{aligned}&\mathbb{E}(\boldsymbol{\varepsilon}_{\boldsymbol{A}_i}\boldsymbol{\varepsilon}^*_{\boldsymbol{C}_i}) = \\ &V_{S_i}^{meas}\boldsymbol{I}_{S_i}^{meas}([\sigma^2_{I_R}(2 - e^{-\sigma^2_{\theta_{I_R}}}) + I_{R_i}^{meas2}(1 - e^{-\sigma^2_{\theta_{I_R}}})]) \\ &+ V_{R_i}^{meas}\boldsymbol{I}_{R_i}^{meas}[\sigma^2_{I_S}(2 - e^{-\sigma^2_{\theta_{I_S}}}) + I_{S_i}^{meas2}(1 - e^{-\sigma^2_{\theta_{I_S}}})]\end{aligned} \tag{C.11}$$

$$\mathbb{E}(\varepsilon_{B_i}\boldsymbol{\varepsilon}^*_{\boldsymbol{C}_i}) = V_{S_i}^{meas}\boldsymbol{I}_{R_i}^{meas*}\sigma^2_{V_S} + V_{R_i}^{meas}\boldsymbol{I}_{S_i}^{meas*}\sigma^2_{V_R} \tag{C.12}$$

And it can readily be shown that $\mathbb{E}(\boldsymbol{\varepsilon}^*_{\boldsymbol{A}_i}\boldsymbol{\varepsilon}_{\boldsymbol{C}_i}) = [\mathbb{E}(\boldsymbol{\varepsilon}_{\boldsymbol{A}_i}\boldsymbol{\varepsilon}^*_{\boldsymbol{C}_i})]^*$ and $\mathbb{E}(\varepsilon_{B_i}\boldsymbol{\varepsilon}_{\boldsymbol{C}_i}) = [\mathbb{E}(\varepsilon_{B_i}\boldsymbol{\varepsilon}^*_{\boldsymbol{C}_i})]^*$.

References

[1] Y. Cong, P. Regulski, P. Wall, M. Osborne, and V. Terzija, "On the use of dynamic thermal-line ratings for improving operational tripping schemes," *IEEE Trans. Power Del.*, vol. 31, no. 4, pp. 1891–1900, 2015.

[2] J. Zhan, C. Chung, and E. Demeter, "Time series modeling for dynamic thermal rating of overhead lines," *IEEE Trans. Power Syst.*, vol. 32, no. 3, pp. 2172–2182, 2017.

[3] T. Van Cutsem and V. Quintana, "Network parameter estimation using online data with application to transformer tap position estimation," in *IEE Proc. C (Gen., Transm. and Dist.)*, vol. 135, no. 1. IET, 1988, pp. 31–40.

[4] A. Abur and A. G. Exposito, *Power system state estimation: theory and implementation*. CRC Press, 2004.

[5] W.-H. Liu, F. F. Wu, and S.-M. Lun, "Estimation of parameter errors from measurement residuals in state estimation (power systems)," *IEEE Trans. Power Syst.*, vol. 7, no. 1, pp. 81–89, 1992.

[6] G. Kusic and D. Garrison, "Measurement of transmission line parameters from SCADA data," in *Power Systems Conference and Exposition, 2004. IEEE PES*. IEEE, 2004, pp. 440–445.

[7] P. Ren, H. Lev-Ari, and A. Abur, "Tracking three-phase untransposed transmission line parameters using synchronized measurements," *IEEE Trans. Power Syst.*, vol. 33, no. 4, pp. 4155–4163, 2017.

[8] J. Zhao, S. Fliscounakis, P. Panciatici, and L. Mili, "Robust parameter estimation of the French power system using field data," *IEEE Trans. Smart Grid*, vol. 10, no. 5, pp. 5334–5344, 2018.

[9] C. Borda, A. Olarte, and H. Diaz, "PMU-based line and transformer parameter estimation," in *Power Systems Conference and Exposition, 2009. PSCE'09. IEEE/PES*. IEEE, 2009, pp. 1–8.

[10] Z. Zhang, N. Kang, and M. Mousavi, "Transformer parameter estimation using terminal measurements," 2017, US Patent App. 15/294,238.

[11] Y. Liao and M. Kezunovic, "Online optimal transmission line parameter estimation for relaying applications," *IEEE Trans. Power Del.*, vol. 24, no. 1, pp. 96–102, 2009.

[12] Y. Liao, "Power transmission line parameter estimation and optimal meter placement," in *IEEE SoutheastCon 2010 (SoutheastCon), Proceedings of the*. IEEE, 2010, pp. 250–254.

[13] Y. Du and Y. Liao, "On-line estimation of transmission line parameters, temperature and sag using PMU measurements," *Elect. Power Syst. Res.*, vol. 93, pp. 39–45, 2012.

[14] D. Ritzmann, P. S. Wright, W. Holderbaum, and B. Potter, "A method for accurate transmission line impedance parameter estimation," *IEEE Trans. Instr. Meas.*, vol. 65, no. 10, pp. 2204–2213, 2016.

[15] D. Ritzmann, J. Rens, P. S. Wright, W. Holderbaum, and B. Potter, "A novel approach to noninvasive measurement of overhead line impedance parameters," *IEEE Trans. Instr. Meas.*, vol. 66, no. 6, pp. 1155–1163, 2017.

[16] P. A. Pegoraro, K. Brady, P. Castello, C. Muscas, and A. von Meier, "Line impedance estimation based on synchrophasor measurements for power distribution systems," *IEEE Trans. Instrum. Meas.*, vol. 68, no. 4, pp. 1002–1013, 2018.

[17] J.-A. Jiang, J.-Z. Yang, Y.-H. Lin, C.-W. Liu, and J.-C. Ma, "An adaptive PMU based fault detection/location technique for transmission lines. I. Theory and algorithms," *IEEE Trans. Power Del.*, vol. 15, no. 2, pp. 486–493, 2000.

[18] Z. Hu and Y. Chen, "New method of live line measuring the inductance parameters of transmission lines based on GPS technology," *IEEE Trans. Power Del.*, vol. 23, no. 3, pp. 1288–1295, 2008.

[19] J. Yang, W. Li, T. Chen, W. Xu, and M. Wu, "Online estimation and application of power grid impedance matrices based on synchronised phasor measurements," *IET Gen., Transm. & Dist.*, vol. 4, no. 9, pp. 1052–1059, 2010.

[20] L. Ding, T. Bi, and D. Zhang, "Transmission line parameters identification based on moving-window TLS and PMU data," in *Advanced Power System Automation and Protection (APAP), 2011 International Conference on*, vol. 3. IEEE, 2011, pp. 2187–2191.

[21] D. Shi, D. J. Tylavsky, K. M. Koellner, N. Logic, and D. E. Wheeler, "Transmission line parameter identification using PMU measurements," *Int. Jour. Elect. Power & Energy Syst.*, vol. 21, no. 4, pp. 1574–1588, 2011.

[22] M. Asprou and E. Kyriakides, "Identification and estimation of erroneous transmission line parameters using PMU measurements," *IEEE Trans. Power Del.*, vol. 32, no. 6, pp. 2510–2519, 2017.

[23] V. Milojević, S. Čalija, G. Rietveld, M. V. Ačanski, and D. Colangelo, "Utilization of PMU measurements for three-phase line parameter estimation in power systems," *IEEE Trans. Instr. Meas.*, vol. 67, no. 10, pp. 2453–2462, 2018.

[24] A. Bendjabeur, A. Kouadri, and S. Mekhilef, "Novel technique for transmission line parameters estimation using synchronised sampled data," *IET Gen., Transm. & Distr.*, 2019.

[25] C. Wang, V. A. Centeno, K. D. Jones, and D. Yang, "Transmission lines positive sequence parameters estimation and instrument transformers calibration based on PMU measurement error model," *IEEE Access*, vol. 7, pp. 145 104–145 117, 2019.

[26] A. Wehenkel, A. Mukhopadhyay, J.-Y. Le Boudec, and M. Paolone, "Parameter estimation of three-phase untransposed short transmission lines from synchrophasor measurements," *IEEE Trans. Instrum. and Meas.*, vol. 69, no. 9, pp. 6143–6154, 2020.

[27] S. S. Mousavi-Seyedi, F. Aminifar, and S. Afsharnia, "Parameter estimation of multiterminal transmission lines using joint PMU and SCADA data," *IEEE Trans. Power Del.*, vol. 30, no. 3, pp. 1077–1085, 2015.

[28] S. Azizi, G. B. Gharehpetian and A. S. Dobakhshari, "Optimal integration of phasor measurement units in power systems considering conventional measurements," *IEEE Trans. Smart Grid*, vol. 4, no. 2, pp. 1113–1121, June 2013.

[29] Y. Wang, W. Xu, and J. Shen, "Online tracking of transmission-line parameters using SCADA data," *IEEE Trans. Power Del.*, vol. 31, no. 2, pp. 674–682, 2016.

[30] C. Li, Y. Zhang, H. Zhang, Q. Wu, and V. Terzija, "Measurement-based transmission line parameter estimation with adaptive data selection scheme," *IEEE Trans. Smart Grid*, vol. 9, no. 6, pp. 5764–5773, 2017.

[31] A. Singhal, H. K. Rathour, P. Agarwal, K. Baba, and S. Soonee, "State estimation at all India level," in *2016 National Power Systems Conference (NPSC)*. IEEE, 2016, pp. 1–6.

[32] Y. Lin and A. Abur, "Robust transformer tap estimation," in *2017 IEEE Manchester PowerTech*. IEEE, 2017, pp. 1–6.

[33] H. Saadat, *Power system analysis*. McGraw-Hill:New York, 1999.

[34] K. S. Miller, "Complex linear least squares," *SIAM Review*, vol. 15, no. 4, pp. 706–726, 1973.

[35] D. Lerro and Y. Bar-Shalom, "Tracking with debiased consistent converted measurements versus EKF," *IEEE Trans. Aeros. and elect. syst.*, vol. 29, no. 3, pp. 1015–1022, 1993.

[36] L. Zanni, A. Derviškadić, M. Pignati, C. Xu, P. Romano, R. Cherkaoui, A. Abur, and M. Paolone, "PMU-based linear state estimation of lausanne subtransmission network: Experimental validation," *Elect. Power Syst. Res.*, vol. 189, p. 106649, 2020.

[37] B. Hall, "On the propagation of uncertainty in complex-valued quantities," *Metrologia*, vol. 41, no. 3, p. 173, 2004.

[38] M. Asprou, E. Kyriakides, and M. Albu, "The effect of variable weights in a WLS state estimator considering instrument transformer uncertainties," *IEEE Trans. Instr. and Meas.*, vol. 63, no. 6, pp. 1484–1495, 2013.

[39] *Instrument transformers - Part 2: Additional requirements for current transformers*, IEC Std. 61 869-2, 2012.

[40] *Instrument transformers - Part 3: Additional requirements for inductive voltage transformers*, IEC Std. 61 869-3, 2012.

[41] N. L. Johnson, A. W. Kemp, and S. Kotz, *Univariate discrete distributions*. John Wiley & Sons, 2005, vol. 444.